



UvA-DARE (Digital Academic Repository)

An unusual pulsar wind nebula associated with PSR B0906-49

Gaensler, B.M.; Stappers, B.W.; Frail, D.A.; Johnston, S.

Published in:
Astrophysical Journal

DOI:
[10.1086/311347](https://doi.org/10.1086/311347)

[Link to publication](#)

Citation for published version (APA):

Gaensler, B. M., Stappers, B. W., Frail, D. A., & Johnston, S. (1998). An unusual pulsar wind nebula associated with PSR B0906-49. *Astrophysical Journal*, 499, L69-L73. DOI: 10.1086/311347

General rights

It is not permitted to download or to forward/distribute the text or part of it without the consent of the author(s) and/or copyright holder(s), other than for strictly personal, individual use, unless the work is under an open content license (like Creative Commons).

Disclaimer/Complaints regulations

If you believe that digital publication of certain material infringes any of your rights or (privacy) interests, please let the Library know, stating your reasons. In case of a legitimate complaint, the Library will make the material inaccessible and/or remove it from the website. Please Ask the Library: <http://uba.uva.nl/en/contact>, or a letter to: Library of the University of Amsterdam, Secretariat, Singel 425, 1012 WP Amsterdam, The Netherlands. You will be contacted as soon as possible.

AN UNUSUAL PULSAR WIND NEBULA ASSOCIATED WITH PSR B0906–49

B. M. GAENSLER,^{1,2} B. W. STAPPERS,^{3,4} D. A. FRAIL,⁵ AND S. JOHNSTON⁶

Received 1998 February 12; accepted 1998 March 23; published 1998 April 22

ABSTRACT

We report on Australia Telescope Compact Array observations of the $\sim 10^5$ yr old pulsar PSR B0906–49. In an image containing only off-pulse emission, we find a weak, slightly extended source coincident with the pulsar’s position, which we argue is best interpreted as a pulsar wind nebula (PWN). A trail of emission extending behind the pulsar aligns with the major axis of the PWN and implies that the pulsar is moving northwest with a projected velocity ~ 60 km s⁻¹, consistent with its scintillation speed. The consequent density we infer for the pulsar’s environment is greater than 2 cm⁻³, so that the PWN around PSR B0906–49 is confined mainly by the high density of its surroundings rather than by the pulsar’s velocity. Other properties of the system such as the PWN’s low luminosity and apparent steep spectrum, and the pulsar’s large characteristic age, lead us to suggest that this nebula is substantially different from other radio PWNe and may represent a transition between young pulsars with prominent radio PWNe and older pulsars for which no radio PWN has been detected. We recommend that further searches for radio PWNe should be made in the same manner: at low frequencies and with the pulsed emission subtracted.

Subject headings: ISM: general — pulsars: individual (PSR B0906–49) — radio continuum: ISM

1. INTRODUCTION

The spin-down observed in most pulsars corresponds to a significant rate of energy loss, which manifests itself primarily in the form of a magnetized wind of relativistic particles (e.g., Rees & Gunn 1974). Under certain conditions, the interaction between this wind and its surroundings is observable, in the form of a pulsar wind nebula (PWN). At radio frequencies, PWNe fall into two basic classes, plerions and bow-shock nebulae: plerions (e.g., Helfand & Becker 1987) are the filled-center components of supernova remnants (SNRs) in which the pulsar wind is confined by the pressure of hot gas in the SNR interior, while bow-shock nebulae are confined by the ram pressure associated with their pulsar’s high velocity (e.g., Frail & Kulkarni 1991; Frail et al. 1996). Both are characterized by significant levels of linear polarization, a centrally peaked morphology, and a flat spectral index ($-0.3 < \alpha < 0$; $S_\nu \propto \nu^\alpha$).

While only a tiny fraction of a pulsar’s spin-down energy goes into producing the radio emission from such nebulae, radio PWNe are valuable diagnostics of the properties of both the wind and the pulsar itself (e.g., Frail et al. 1996). Insight into the workings of such PWNe is limited by the fact that only six pulsars, all with ages $\leq 10^5$ yr, have associated radio PWNe (Frail & Scharringhausen 1997, hereafter FS97). Attempts to detect radio nebulae around older pulsars have so far been unsuccessful (e.g., Cohen et al. 1983).

In an attempt to increase the sample of radio PWNe, FS97

used the Very Large Array at 8.4 GHz to search for PWNe around 35 pulsars of high spin-down luminosity and/or velocity, but they found no new PWNe down to a surface brightness $T_b \sim 1.2$ K. They concluded that only young, energetic pulsars produce observable radio nebulae and that the properties of a pulsar’s wind may change as the pulsar ages. However, a weak, compact, or steep-spectrum nebula is difficult to detect using the approach of FS97, because the nebula is “hidden” by the emission from its associated pulsar. This has motivated us to attempt an alternative strategy for finding radio PWNe, whereby visibilities are recorded at high time resolution so that off-pulse images can be produced. The full results of this program are described elsewhere (Stappers et al. 1998); here we report on the discovery of an unusual PWN associated with PSR B0906–49.

PSR B0906–49 ($l = 270^\circ.3$, $b = -1^\circ.0$) is a 107 ms pulsar (D’Amico et al. 1988) whose characteristic age $\tau_c = 112,000$ yr and spin-down luminosity $\dot{E} = 4.9 \times 10^{35}$ ergs s⁻¹ place it among the 5% youngest and most energetic of all pulsars. H I absorption has yielded distances to the pulsar in the ranges 2.4–6.7 kpc (Koribalski et al. 1995) and 6.3–7.7 kpc (Saravanan et al. 1996), while a distance estimate using the pulsar’s dispersion measure (Taylor & Cordes 1993) is $6.6_{-0.9}^{+1.3}$ kpc. In future discussions, we assign it a distance $7d_7$ kpc. The pulse profile shows a strong main pulse and a weaker interpulse, both of which are $\sim 90\%$ linearly polarized (Wu et al. 1993; Qiao et al. 1995). Scintillation measurements imply a transverse velocity for the pulsar of $\sim 50d_7^{1/2}$ km s⁻¹ (Johnston, Nicastro, & Koribalski 1998).

2. OBSERVATIONS

Observations of PSR B0906–49 were carried out with the Australia Telescope Compact Array (ATCA) and are described in Table 1. In each observation, two continuum frequencies were observed simultaneously with 32 4 MHz channels across each; all four Stokes parameters were recorded. All observations were carried out in pulsar-gating mode, in which visibilities were sampled at a time resolution of 3.3 ms (32 bins

¹ Astrophysics Department, School of Physics A29, University of Sydney, NSW 2006, Australia; b.gaensler@physics.usyd.edu.au.

² Australia Telescope National Facility, CSIRO, P.O. Box 76, Epping, NSW 2121, Australia.

³ Astronomical Institute “Anton Pannekoek,” University of Amsterdam, Kruislaan 403, 1098 SJ Amsterdam, The Netherlands; bws@astro.uva.nl.

⁴ Mount Stromlo and Siding Spring Observatories, Institute of Advanced Studies, Australian National University, Private Bag, Weston Creek Post Office, ACT 2611, Australia.

⁵ National Radio Astronomy Observatory, P.O. Box O, 1003 Lopezville Road, Socorro, NM 87801; dfrail@nrao.edu. NRAO is a facility of the NSF operated under cooperative agreement by Associated Universities, Inc.

⁶ Research Centre for Theoretical Astrophysics, University of Sydney, NSW 2006, Australia; s.johnston@physics.usyd.edu.au.

TABLE 1
ATCA OBSERVATIONS OF PSR B0906–49

DATE (1997)	ARRAY CONFIGURATION	MAXIMUM BASELINE (m)	TIME ON-SOURCE (hr)	CENTER FREQUENCY (GHz)	
				1	2
May 12	6.0B	5969	12	1.344	2.240
Aug 17	1.5B	1286	12	1.344	2.240
Nov 6	6.0C	6000	11	1.216	1.728

per period) and then folded at the apparent pulse period. These summed visibilities were then recorded every 40 s.

The flux density scale of the observations was determined by observations of PKS B1934–638, while polarization and antenna gains were calibrated using observations of PKS B0823–500 every 45 minutes. The data were edited and calibrated using the MIRIAD package and then de-dispersed at a dispersion measure of 179 pc cm^{-3} . The resultant smearing due to the finite channel width was in all cases no more than one time bin. At each frequency, the field of interest was imaged, deconvolved using 10^4 iterations of the CLEAN algorithm, and then convolved with a Gaussian beam of dimensions corresponding to the diffraction limit.

3. RESULTS

In Figure 1a, we show a 1.3 GHz image of the region surrounding the pulsar, using all time bins from the 1997 May and August observations. An adjacent H II region (Green, Cram, & Large 1998) contributes considerable extended emission, which we discard by imaging using only u - v spacings greater than $1 \text{ k}\lambda$. The pulsar is apparent as an unresolved source at position R.A. (J2000) $09^{\text{h}}08^{\text{m}}35^{\text{s}}$, decl. (J2000) $-49^{\circ}13'06''$, in agreement with its timing position (D'Amico et al. 1988). Extracting the time dependence of the data at these coordinates from the visibilities gives the profile shown in Figure 2, clearly showing the main pulse and interpulse. Similar profiles are obtained at other frequencies: flux densities for the pulsar (including any coincident unpulsed emission) are given in Table 2. An unrelated source, ATCA J090850–491301, can be seen 2.5 to the east of the pulsar, with flux densities also listed in Table 2.

Figure 1b shows the same field as in Figure 1a, but generated by using only time bins in which there is no discernible pulsed emission. A weak source can now be seen at the position of the pulsar. While the pulsar's emission is well fitted by a Gaussian corresponding to a point source, a fit to this weaker source shows it to be extended, with dimensions $15''0 \times 10''0$ at a position angle (P.A.) of $315^{\circ} \pm 10^{\circ}$ (north through east). After correction for bandwidth depolarization, the source is less than $\sim 50\%$ polarized. The position of its peak agrees with that of PSR B0906–49 to $0''.6$ in R.A. and to $0''.4$ in decl.

The flux density of the off-pulse source as a function of frequency is detailed in Table 2. In observations at 1.7 and 2.2 GHz, the source was not detected, despite being detected simultaneously at each epoch at a lower frequency. For non-detections, we quote upper limits to the flux density derived using the method of Green & Scheuer (1992). This involves adding to the data simulated sources of the same dimensions as the off-pulse source, increasing the flux density until the simulated source is distinguishable above the noise. The upper

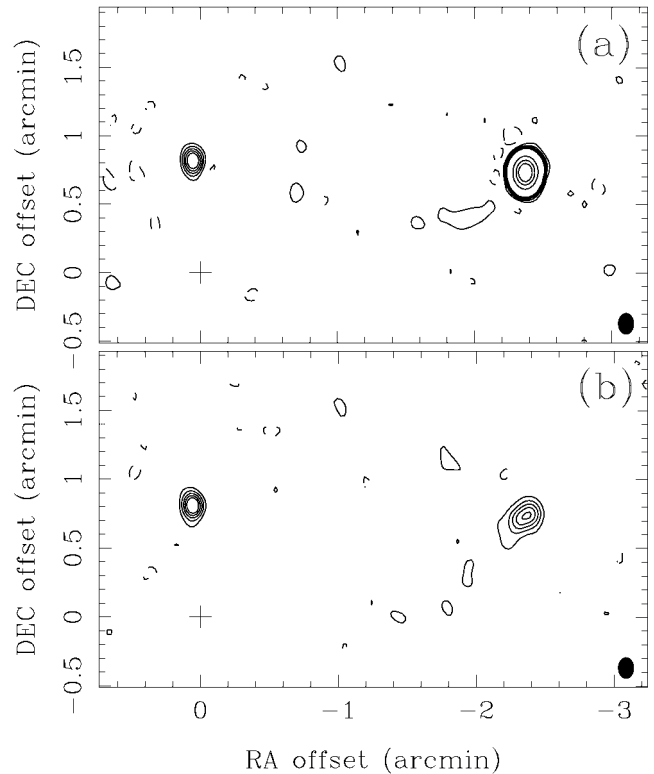


FIG. 1.—The 1.3 GHz images (1997 May and August data combined) of a region surrounding PSR B0906–49, with baselines shorter than $1 \text{ k}\lambda$ excluded: (a) all time bins; (b) off-pulse bins only. The rms noise in the images is limited by confusion to $0.06 \text{ mJy beam}^{-1}$ ($T_b = 0.7 \text{ K}$). The contours are at -0.15 (broken), 0.15 , 0.3 , 0.45 , 0.6 , 0.75 , 5 , 10 , and 15 mJy beam^{-1} . The resolution (as shown at the bottom right of each image) is $9''.4 \times 7''.0$, P.A. = 0° . The cross indicates the position of the phase center, R.A. (J2000) $09^{\text{h}}08^{\text{m}}50^{\text{s}}$, decl. (J2000) $-49^{\circ}13'50''$.

limits quoted in Table 2 are conservative, being twice the values at which a simulated source could be discerned.

A 1.3 GHz off-pulse image from the 1997 May 12 data, made using all baselines, is shown in Figure 3. As well as ATCA J090850–491301 and the off-pulse source, a faint trail of emission can be seen, extending ~ 3.5 southeast from the

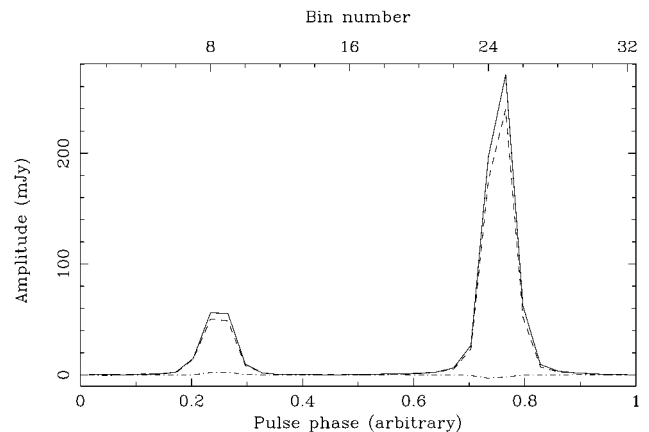


FIG. 2.—Pulse profile of B0906–49 at 1.3 GHz. The solid, dashed, and dot-dashed lines represent total, linearly polarized, and circularly polarized intensity, respectively. The profile is 90% linearly and 3% circularly polarized, values close to those determined in previous measurements.

TABLE 2
FLUX DENSITIES AND SENSITIVITY AS A FUNCTION OF FREQUENCY

FREQUENCY (GHz)	FLUX DENSITY (mJy) ^a			RMS NOISE ^a (mJy beam ⁻¹)
	PSR B0906–49	PWN B0906–49	ATCA J090850–491301	
1.216	22 ± 2	1.4 ± 0.3	1.0 ± 0.2	0.14
1.344	25 ± 2	1.5 ± 0.3	1.1 ± 0.2	0.06
1.728	16 ± 2	<1.0	1.0 ± 0.2	0.07
2.240	14 ± 2	<1.0	1.0 ± 0.2	0.06

NOTE.—On the basis of simultaneous dual-frequency observations, we compute an approximate spectral index for the pulsar of $\alpha \sim -1$. The differences in the pulsar’s flux density between the three observations are most likely due to refractive scintillation.

^a 1 Jy = 10^{-26} W m⁻² Hz⁻¹.

pulsar’s position, broadening with increasing distance from it before abruptly terminating. The apex of the trail coincides with the position of the pulsar, and the position angle defined by the bisection of the trail’s two flanks is consistent with the direction along which the off-pulse source is extended. The flux density of the trail is ~ 7 mJy. In the 1.3 GHz data from the 1997 August 17 observations, the trail is just visible amid confusing thermal emission. The trail was not detected in 1.2 GHz observations (which were severely affected by interference), nor was it seen at 1.7 or 2.2 GHz (as for the off-pulse source). While the inclusion of short baselines produces a great deal of confusing structure, no other feature resembling the trail is seen in any part of the field in any observation.

An H α observation of the region (Buxton, Bessell, & Watson 1998) shows no emission that can be associated with any radio-emitting source, a result that can be attributed to a foreground dark cloud (Hartley et al. 1986).

4. DISCUSSION

We consider four possible explanations for the weak source coincident with PSR B0906–49: positional coincidence with an unrelated source, a compact SNR, emission from the pulsar itself, or a pulsar wind nebula associated with the pulsar.

At $\lambda = 20$ cm, extragalactic source counts (e.g., Windhorst et al. 1985) imply a probability $\sim 10^{-5}$ of finding a background

radio source of flux density greater than 1 mJy within 1" of the pulsar, allowing us to rule out a coincidental alignment. We estimate that positional coincidence with an unrelated Galactic source is also unlikely.

The source under consideration may be a compact SNR, in the form of either a shell (Green 1985) or a plerion (Helfand et al. 1989). However, a shell or plerion of age $\tau_c \approx 10^5$ yr and radius $\approx 0.3d_7$ pc, as required here, results in an improbably high ($>10^8$ cm⁻³) density for the surrounding medium. No other emission is seen in the region that might correspond to a more extended SNR (Duncan et al. 1995; Green et al. 1998), and we presume it to have dissipated.

Although we took care to create an image using only off-pulse bins, it is impossible to exclude the possibility that Figure 1b still contains some flux from the pulsar, in the form of either unpulsed emission or a further weak component to the pulse profile. Our main argument against such interpretations is that the off-pulse source appears extended. Although the source is too weak to fit into the u - v plane, its extension and position angle are quite different from those of the synthesized beam and are visible at all reasonable contour levels. It is difficult to see how the presence of noise, sidelobes, or other artifacts could artificially create such an appearance. The extension is not directed toward the phase center and so cannot be accounted for by bandwidth smearing. Nor is there evidence for significant time variability in the pulsar’s flux, which might also mimic an extended source (and in any case would cause the pulsar itself to appear similarly extended). The source is evident in repeated observations and persists when imaging various subsets of the off-pulse component of the pulse profile. The off-pulse source also lacks the high fractional linear polarization observed for the pulsar. We thus conclude that it is unlikely that the source represents emission from the pulsar itself.

The remaining possibility is that this source represents synchrotron emission from a pulsar wind nebula associated with PSR B0906–49. The observed elongation of the PWN suggests that it is a bow-shock nebula, an interpretation supported by the trail’s morphology and its alignment with the PWN’s major axis. We interpret the trail as a synchrotron wake⁷ extending behind the pulsar, whose inferred direction of motion is thus along P.A. = 315°. This wake is analogous to similar radio structures seen trailing behind PSRs B1757–24 (Frail & Kul-karni 1991) and B1853+01 (Frail et al. 1996) and behind the X-ray binary Circinus X-1 (Stewart et al. 1993).

By demanding that the pulsar has traversed the trail’s length in its lifetime (which we equate to τ_c in all further discussion), we determine a velocity $v \geq 60d_7/\sin i$ km s⁻¹, where i is the

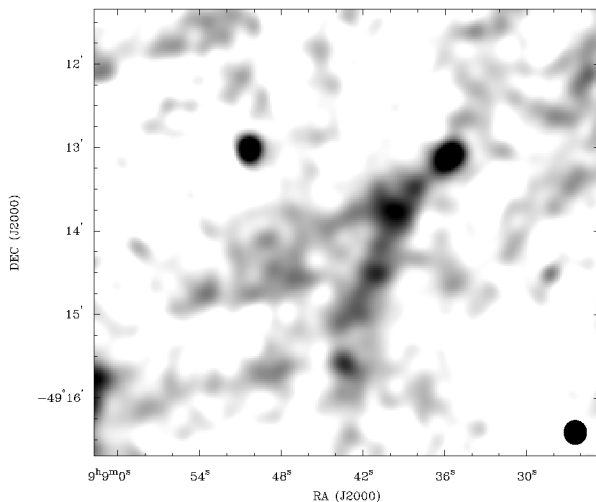


FIG. 3.—A 1.3 GHz image of off-pulse emission from the 1997 May 12 data, using all baselines. The gray-scale range is 0–0.5 mJy beam⁻¹, and the resolution (indicated at bottom right) is 17".7 × 16".6, P.A. = 5°. The rms noise is 0.12 mJy beam⁻¹.

⁷ In further discussion, the “PWN” corresponds to the compact off-pulse source, while the “trail” corresponds to the extended emission to the southeast.

inclination of the pulsar's direction of motion to the line of sight. The well-defined edge to the trail in the southeast suggests that the lack of emission beyond this point corresponds to a change in conditions rather than to synchrotron losses (which are most likely negligible over the pulsar's lifetime in any case). Given the agreement between the lower limit on v and the scintillation velocity (Johnston et al. 1998), we propose that the pulsar was born at the base of the trail and adopt a velocity $v = 60v_{60}/\sin i$ km s⁻¹. The implied proper motion of $1.8v_{60}d_7^{-1}$ mas yr⁻¹ is too small to be measured directly but could be constrained or ruled out through pulsar timing or the VLBI.

The pulsar wind flows freely from the pulsar until it encounters a reverse shock at radius r_s (e.g., Cordes 1996). The location of this shock is unresolved in our data, and from our highest resolution data, we estimate $r_s < 10^{17}d_7$ cm. We assume that all the pulsar's spin-down luminosity goes into the pulsar wind; upper limits to its γ -ray flux (Thompson et al. 1994) make this a reasonable assumption to within a factor of 2. Thus, equating the energy density of the pulsar wind, $\dot{E}/4\pi r_s^2 c$, with the ram pressure due to the pulsar's motion, ρv^2 , we find an ambient (hydrogen) density $n > 2(d_7 v_{60}/\sin i)^{-2}$ cm⁻³, significantly higher than for the general interstellar medium. A distance greater than 7 kpc is inconsistent with the pulsar's H I absorption; thus, only if the pulsar's velocity is significantly greater than 60 km s⁻¹ can this discrepancy be reconciled. If we adopt the lower distance limit determined by Koribalski et al. (1995) and adjust the pulsar velocity accordingly, the required density rises to $n > 70/\sin i$ cm⁻³. We note that the CO survey of Grabelsky et al. (1987) shows molecular material in the direction of PSR B0906–49, at velocities corresponding to the range determined for the pulsar from H I absorption. Thus, PWN B0906–49 appears to be a bow-shock PWN in which the main contribution to the confining ram pressure appears to be the density of surrounding material rather than the pulsar's high velocity. While there are other instances of bow-shock PWNe around low-velocity pulsars (see Cordes 1996), PSR B0906–49 is the only case in which the PWN has been detected at radio frequencies.

The spectral index of PWN B0906–49 is poorly determined by the available data, but assuming a single power law over the observed range implies $-3.5 \lesssim \alpha \lesssim -0.7$. This is significantly steeper than for filled-center SNRs⁸ and for the six other known radio PWNe; we note that such a nebula would not have been detected by the 8.4 GHz search of FS97. For $\alpha = -1$, the integrated radio luminosity of the PWN is $L_R \approx 10^{30}d_7^2$ ergs s⁻¹, corresponding to an efficiency $\epsilon_R \equiv L_R/\dot{E} \approx 2 \times 10^{-6}d_7^2$. These values of L_R and ϵ_R are significantly lower than for any other radio PWN (see FS97). Of pulsars powering such nebulae, only PSR B1853+01 has a (slightly) lower \dot{E} .

The unusual spectrum of PWN B0906–49 may relate to a decrease in the efficiency of shock acceleration resulting from enhanced densities and reduced shock velocities (Pineault et al. 1997). If a significant component of the radio emission is due to electrons accelerated at the shock front between the pulsar wind and its surroundings, the high density and low velocity we have proposed for this source might explain its steep spectrum and low luminosity. Alternatively, FS97 have

argued that older, less energetic pulsars do not produce observable radio nebulae, and a simple explanation for both their and our observations is that the intrinsic spectrum of injected electrons steepens with age. Apart from PSR B1951+32 ($\tau_c = 107,000$ yr), B0906–49 is at least 5 times older than any other pulsar associated with a radio PWN. While PSR B1951+32 is only slightly younger than PSR B0906–49, the former system represents a complicated interaction between the pulsar and its associated SNR (Shull, Fesen, & Saken 1989), and it is difficult to separate the contribution of the pulsar wind from that of the supernova shock.

5. CONCLUSION

Using pulsar-gating observations at $\lambda = 20$ cm, we have found an off-pulse, slightly extended source coincident with PSR B0906–49, which we interpret as a faint pulsar wind nebula. An associated trail implies a projected velocity for the pulsar of ~ 60 km s⁻¹ along a position angle of 315°. The system is unusual in several ways:

1. The nebula has a lower luminosity and steeper spectrum than any other radio PWN yet discovered.
2. PSR B0906–49 is older than any other pulsar known to power a radio PWN, while only PSR B1853+01 has a lower spin-down luminosity.
3. The PWN appears to be generated by a slow (~ 60 km s⁻¹) pulsar moving through a dense (> 2 cm⁻³) medium.

Thus, PWN B0906–49 appears to be very different from other radio PWNe. To account for this, we propose either that the low velocity and high density inhibit shock acceleration or that the particle spectrum injected by a pulsar into its PWN steepens with age. In the latter case, PWN B0906–49 may be in transition between the high-luminosity, flat-spectrum PWNe seen around young pulsars and the undetectable radio PWNe seen around older pulsars. We note that PWNe of low flux density and steep spectrum were heavily selected against in FS97's ungated, high-frequency observations. We therefore recommend that future searches, particularly around intermediate-age pulsars, should be made in the same manner: at low frequencies and by imaging only the off-pulse emission. A collection of PWNe produced under a variety of conditions still needs to be accumulated before we can fully understand how the radio emission from a PWN is produced and how it depends on the properties of its pulsar.

We thank the ATNF Time Assignment Committee for generously assigning an extra configuration, Mike Bessell and Michelle Buxton for providing H α data on the region, and Dick Manchester for supplying the pulsar ephemeris. B. M. G. acknowledges the support of an Australian Postgraduate Award, while B. W. S. received support from an ANU Ph.D. Scholarship and the ATNF Higher Degree Programme. The Australia Telescope is funded by the Commonwealth of Australia for operation as a National Facility operated by CSIRO. This research has made use of NASA's Astrophysics Data System Abstract Service and of the SIMBAD database, operated at CDS, Strasbourg, France.

⁸ See A Catalogue of Galactic Supernova Remnants (1996 August version) (Cambridge: MRAO) (<http://www.mrao.cam.ac.uk/surveys/snrns/>) by D. A. Green.

REFERENCES

- Buxton, M., Bessell, M., & Watson, B. 1998, *Publ. Astron. Soc. Australia*, 15, 24
- Cohen, N. L., Cotton, W. D., Geldzahler, B. J., & Marcaide, J. M. 1983, *ApJ*, 264, 273
- Cordes, J. M. 1996, in *ASP Conf. Ser. 105, Pulsars: Problems and Progress*, IAU Colloq. 160, ed. S. Johnston, M. A. Walker, & M. Bailes (San Francisco: ASP), 393
- D'Amico, N., Manchester, R. N., Durdin, J. M., Stokes, G. H., Stinebring, D. R., Taylor, J. H., & Brissenden, R. J. V. 1988, *MNRAS*, 234, 437
- Duncan, A. R., Stewart, R. T., Haynes, R. F., & Jones, K. L. 1995, *MNRAS*, 277, 36
- Frail, D. A., Giacani, E. B., Goss, W. M., & Dubner, G. 1996, *ApJ*, 464, L165
- Frail, D. A., & Kulkarni, S. R. 1991, *Nature*, 352, 785
- Frail, D. A., & Scharringhausen, B. R. 1997, *ApJ*, 480, 364 (FS97)
- Grabelsky, D. A., Cohen, R. S., Bronfman, L., Thaddeus, P., & May, J. 1987, *ApJ*, 315, 122
- Green, A. J., Cram, L. E., & Large, M. I. 1998, *ApJ*, submitted
- Green, D. A. 1985, *MNRAS*, 216, 691
- Green, D. A., & Scheuer, P. A. G. 1992, *MNRAS*, 258, 833
- Hartley, M., Manchester, R. N., Smith, R. M., Tritton, S. B., & Goss, W. M. 1986, *A&AS*, 63, 27
- Helfand, D. J., & Becker, R. H. 1987, *ApJ*, 314, 203
- Helfand, D. J., Velusamy, T., Becker, R. H., & Lockman, F. J. 1989, *ApJ*, 341, 151
- Johnston, S., Nicastro, L., & Koribalski, B. 1998, *MNRAS*, in press
- Koribalski, B. S., Johnston, S., Weisberg, J., & Wilson, W. 1995, *ApJ*, 441, 756
- Pineault, S., Landecker, T. L., Swerdlyk, C. M., & Reich, W. 1997, *A&A*, 324, 1152
- Qiao, G. J., Manchester, R. N., Lyne, A. G., & Gould, D. M. 1995, *MNRAS*, 274, 572
- Rees, M. J., & Gunn, J. E. 1974, *MNRAS*, 167, 1
- Saravanan, T. P., Deshpande, A. A., Wilson, W., Davies, E., McCulloch, P. M., & McConnell, D. 1996, *MNRAS*, 280, 1027
- Shull, J. M., Fesen, R. A., & Saken, J. M. 1989, *ApJ*, 346, 860
- Stappers, B. W., Gaensler, B. M., Johnston, S., & Frail, D. A. 1998, in preparation
- Stewart, R. T., Caswell, J. L., Haynes, R. F., & Nelson, G. J. 1993, *MNRAS*, 261, 593
- Taylor, J. H., & Cordes, J. M. 1993, *ApJ*, 411, 674
- Thompson, D. J., et al. 1994, *ApJ*, 436, 229
- Windhorst, R. A., Miley, G. K., Owen, F. N., Kron, R. G., & Koo, D. C. 1985, *ApJ*, 289, 494
- Wu, X., Manchester, R. N., Lyne, A. G., & Qiao, G. 1993, *MNRAS*, 261, 630